

Magnetic resonance in spin glasses: $\text{Fe}_8\text{Ni}_{72}\text{P}_{20}$ and $\text{Fe}_{10}\text{Ni}_{70}\text{P}_{20}$

M.-K. Hou and M. B. Salamon

Department of Physics, University of Illinois at Urbana—Champaign, 1110 West Green Street, Urbana, Illinois 61801

T. A. L. Ziman

Institut Laue-Langevin, Boîte Postale 156X, F-38042 Grenoble, France

(Received 24 April 1984)

An ESR study on amorphous $\text{Fe}_8\text{Ni}_{72}\text{P}_{20}$ and $\text{Fe}_{10}\text{Ni}_{70}\text{P}_{20}$ spin-glass alloys was performed at 1.1 and 9.3 GHz. The line shape, at both frequencies, shows progressive distortion as the temperature is reduced. We use an improved dynamical model to fit the distorted line shapes and demonstrate that there is a tendency for the relaxation rate to vanish as T_f is approached. In the spin-glass regime, we also find a shift in resonance position in addition to the dynamical one, which is due to the existence of a static anisotropy field in the spin-glass state. The anisotropic energy $K(T)$ is found to be proportional to $(1 - T/T_f)$.

I. INTRODUCTION

A key aspect of the spin-glass transition is the onset of a slow time decay of spin correlations without a corresponding change in spatial decay. Electron spin resonance (ESR) measurements on spin glasses reflect this through an increase in linewidth and a shift in resonant field as the temperature is reduced toward T_f .¹ Previously, we demonstrated² that both the broadening and shift could be explained by exchange narrowing of a spin-nonconserving interaction above T_f . More recently, similar conclusions³ have been reached for ESR results on AgMn. Both our previous result and its extension by Levy *et al.*⁴ use the standard Kawasaki-Mori theory⁵ of resonance line shape. The latter authors⁴ have considered a Dzyaloshinsky-Moriya interaction as the source of the resonance width and improved the decoupling of four-spin correlation functions. However, the conclusions remain unchanged: As T_f is approached, spin fluctuations slow, leading to a dynamical shift in resonance position and broadening of the line.

By contrast, the ESR behavior far below T_f has been studied by Schultz *et al.*⁶ They associate the resonance position in CuMn with the existence of static anisotropy fields and a remanent magnetization. Using a phenomenological equation of motion, they could explain the position of their ESR lines, and predicted a second resonance mode when the anisotropy frequency $\gamma[K(T)/\chi]^{1/2}$ exceeds the spectrometer frequency ω . Here, $K(T)$ is the temperature-dependent anisotropy, χ the susceptibility, and γ the gyromagnetic ratio. The phenomenological model has been placed on more solid theoretical foundations by Henley *et al.*⁷ and by Saslow.⁸ It has remained unclear how to connect the low-temperature anisotropy model with the high-temperature exchange-narrowing picture.⁹

Naively, one might expect the Lorentzian, exchange-narrowed line to evolve to Gaussian shape as the spin dynamics slow, finally giving an inhomogeneously broadened line. In fact, the line shape becomes strongly

distorted (neither Lorentzian nor Gaussian), even above T_f . The problem, as first pointed out by Kubo and Toyabe,¹⁰ lies with the usual assumptions leading to the Kawasaki-Mori formalism, which are invalid when the modulation is slow and the spin-nonconserving field is larger than the Zeeman field. The distinction between secular and nonsecular terms is lost, and the Zeeman splitting becomes a perturbation on the static splitting induced by the random, nonconserving field.

In this paper, we report ESR measurements of two amorphous spin glasses, $\text{Fe}_8\text{Ni}_{72}\text{P}_{20}$ and $\text{Fe}_{10}\text{Ni}_{70}\text{P}_{20}$ at 1.1 and 9.3 GHz spectrometer frequencies. A form of the Kubo-Toyabe model¹¹ is used to make detailed fits to the resonance lines. In addition to the dynamic effect of random local fields, to explain the line shift in the spin-glass regime requires the presence of a static anisotropy field along the applied field. Unlike the analysis of Schultz *et al.*,⁶ inclusion of the dynamical effects accounts for all of the shift in resonance position above T_f and the static anisotropy field is found to vanish at T_f , as it should if it follows the spin-glass order parameter. From the data, we can determine the parameters of Kubo-Toyabe model; these show clearly the decrease in relaxation rate for random fields, but give nonzero rate at T_f . A brief report of the 9.3 GHz data was published previously.¹²

II. EXPERIMENT

The freezing temperatures of $\text{Fe}_8\text{Ni}_{72}\text{P}_{20}$ and $\text{Fe}_{10}\text{Ni}_{70}\text{P}_{20}$ are 18 and 23 K, respectively, determined from the position of the cusp in the dc magnetic susceptibility at low field.¹³ ESR measurements at 9.3 GHz were performed with a conventional cold-finger ESR spectrometer, and at 1.1 GHz with a cold-finger strip-line resonant cavity. Ribbon samples of these alloys were cut to 1 or 2 cm lengths and mounted in the center of both ESR spectrometers. The sample could be rotated to have the applied field either parallel or perpendicular to the face of the ribbon. As noted above, the line shape shows progres-

sive distortions at reduced temperature. These distortions give rise to spurious peaks at low field when the usual derivative method is used; consequently, data were taken without field modulation. To minimize line-shape changes due to skin-effect mixing, the samples were thinned to 10 μm , approximately equal to the microwave skin depth, by mechanical polishing. The mixing ratio of the real part of the susceptibility to the imaginary part in the data at 9.3 GHz is 0.45:1 for $\text{Fe}_8\text{Ni}_{72}\text{P}_{20}$ and 0.47:1 for $\text{Fe}_{10}\text{Ni}_{70}\text{P}_{20}$, while at 1.1 GHz, it is 0.2:1 for $\text{Fe}_8\text{Ni}_{72}\text{P}_{20}$ and 0.18:1 for $\text{Fe}_{10}\text{Ni}_{70}\text{P}_{20}$, approximately the expected \sqrt{f} dependence. These ratios are determined from high-temperature ESR data and are taken to be temperature independent, as expected from the small change in resistivity of both samples over the temperature range of interest.¹⁴ Other groups¹⁵ have noted the need to change the mixing ratio substantially near T_f . Rather than a change in skin depth, this approximately accounts for the changes in line shape that we report in detail here. To test that the distortions are not due to an inhomogeneous demagnetization field at the edge of the sample, we plated copper on the sample ends, but observed no change in line shape. Because these samples have very small offsets in their hysteresis loops, the interesting problem⁶⁻⁸ of resonance modes in the field-cooled configuration does not arise.

The resonance field H_0 was determined by measuring the resonance in both the parallel and perpendicular configurations. For the applied field normal to the face of the sample, the observed resonance field $H_{r\perp}$ is related to the true resonance field H_R by¹⁶

$$H_{r\perp} = H_R + 4\pi M_{\perp}, \quad (1)$$

where M_{\perp} is the magnetization in the internal field of the sample, i.e., $M_{\perp} = M(H_R)$. Parallel to the sample plane, we have

$$H_R = [H_{r\parallel}(H_{r\parallel} + 4\pi M_{\parallel})]^{1/2}, \quad (2)$$

where $M_{\parallel} = M(H_{r\parallel})$. Defining $a = M_{\parallel}/M_{\perp}$, we can combine Eqs. (1) and (2) to get

$$H_R = \frac{1}{2} \{ [(4 + a^2)H_{r\parallel}^2 + 4aH_{r\parallel}H_{r\perp}]^{1/2} - aH_{r\parallel} \}. \quad (3)$$

In the paramagnetic phase $T \gg T_f$, the resonance field H_R derived from the data at 9.3 GHz has a constant value, $H_R \cong 3.340$ kOe, corresponding to a g value of 2.0. As temperature is reduced, H_R begins to decrease near the freezing temperature and continues to decrease in the spin-glass regime. As shown in Fig. 1, this is accompanied by a progressive change in line shape: The exchange-narrowed line at $T \gg T_f$ shifts and broadens as temperature is decreased toward T_f . It becomes asymmetric, and finally develops an absorption at zero field below T_f . Under such conditions, the maximum in the absorption can no longer be taken to be the field for resonance nor can (3) be applied. In the data at 1.1 GHz, the linewidth is much larger than the resonance field, and the negative frequency contribution is very strong. In this regime, H_R just represents the position of maximum intensity and decreases very rapidly with decreasing temperature, approaching zero near T_f . The contribution of the resonance line for negative frequency (opposite polariza-

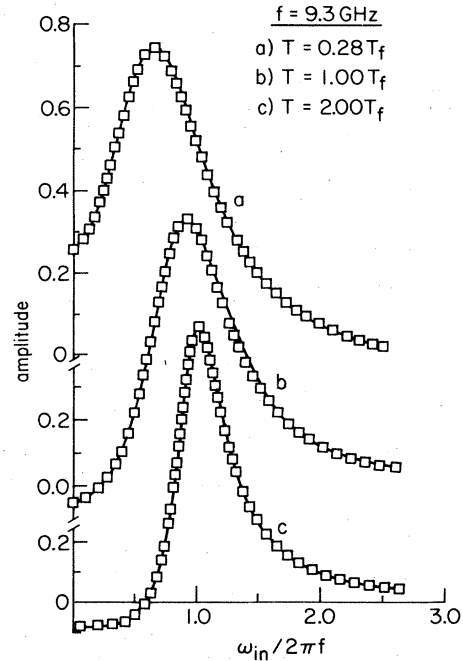


FIG. 1. Plotted as a function of internal frequency $\omega_{in} = \gamma H_{in}$, the line shape at 9.3 GHz, c , is Lorentzian at $T \gg T_f$; becomes distorted, b , around $T = T_f$, and absorption at zero field, a , develops for $T < T_f$. The squares indicate the data points and the solid line, the theoretical line shape.

tion) is significant over the entire temperature range of interest. However, we can still see in Fig. 2 the progressive changes in line shape as temperature is reduced. In the presence of such severe distortions in line shape at both frequencies, linewidth measurements—especially these involving peak-to-peak values from the derivative method—lose their meaning. Therefore, we have made least-square fits of the data to an improved model, described below.

In the particular configuration the absorption line is slightly broader than that in the parallel configuration; the difference is due to the fact that the demagnetization field in the samples is along the applied field for perpendicular configuration but perpendicular for parallel configuration. When the demagnetization field is along the applied field, it shifts the resonance to high field by stretching the field scale. Similarly, when the demagnetization field is perpendicular to the applied field, it moves the line to lower field and also compresses the scale. The distortion of the field scale gives different widths of the line in field for the same relaxation rate. Therefore, the magnetization $M(H, T)$ of both samples and data taken in the perpendicular configuration are used to obtain the lines on an internal field scale. The relation between internal field H_{in} and external field H_{out} is given by the usual equation

$$H_{out} = H_{in} + 4\pi M(H_{in}, T). \quad (4)$$

In the simplest form of the exchange-narrowing model, the linewidth ΔH and g factor are both governed by

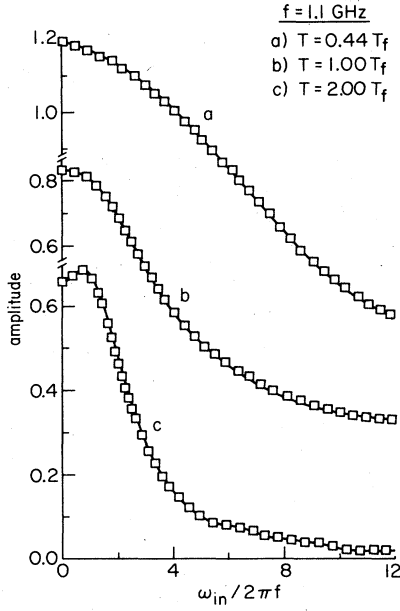


FIG. 2. Line shape at 1.1 GHz shows a progressive change with temperature. Line shape at $T \gg T_f$ (c) is narrowed and the maximum intensity position is at nonzero internal field; it becomes broader, b at $T = T_f$ and the maximum intensity position moves to zero field and the line shape becomes much broader, a for $T < T_f$.

dynamical effects, and are given roughly by $\gamma\Delta H \cong \omega_d^2 \tau_{\text{eff}} / \chi$ and $\Delta g/g \cong \omega_d^2 \tau_{\text{eff}}^2 / \chi$. Here ω_d/γ is the strength of the field causing the broadening while τ_{eff} is its correlation time. For spin glasses, the susceptibility has no critical behavior near T_f , but we expect⁴ slowing down of dynamical effects; that is, an increase in τ_{eff} . We

previously used such arguments to explain the simultaneous increase in ΔH and Δg . However, as noted above, these expressions are only valid for $\omega_d \tau_{\text{eff}} \ll 1$. For slow modulation and low applied fields, a more complete treatment is required.

III. SLOW-MODULATION THEORY

In order to calculate line shapes in the slow-modulation regime, we have followed the theory of Kubo and Toyabe,¹⁰ as modified by Hayano *et al.*¹¹ In this model, spins precess in the resultant of an applied field, parallel to the z axis, and random field $\vec{H}(t)$. The response is averaged over the distribution of random variables $\vec{H}(t)$, which models the effects of spin-nonconserving terms in the Hamiltonian. The instantaneous values of $\vec{H}(t)$ are distributed according to a Gaussian of width Δ/γ and zero mean. Thus, this model can apply rigorously only to the zero-field cooled state. The correlations are assumed to decay exponentially with rate constant ν . Then, the correlation function takes the form

$$\langle \vec{H}(t+\tau) \cdot \vec{H}(\tau) \rangle = 3(\Delta/\gamma)^2 \exp(-\nu t), \quad (5)$$

where γ is the gyromagnetic ratio. The assumption of exponential decay of the random field autocorrelation function makes this model only approximately valid for spin-glasses, where power-law decays are expected.¹⁷

The ESR resonance spectrum $I_{xx}(\omega)$ is proportional to the real part of the relaxation function $F_{xx}(\omega, \nu)$, which is the Fourier transform of the correlation function of the total spin $G_{xx}(t, \nu)$. In the static ($\nu=0$) limit, we define $I_{xx}(\omega) \propto \text{Re} F(\omega, \nu=0) \equiv \text{Re} f_{xx}^0(\omega)$, and $G_{xx}(t, \nu=0) = g_{xx}(t)$; the latter is determined from the correlation function of the total spin $\vec{\sigma}$. In the static $\nu=0$ limit, the fields are frozen and we obtain, as by Hayano *et al.*,

$$g_{zz}(t) \equiv \langle \sigma_z(t) \sigma_z(0) \rangle = 1 - (2\Delta^2/\omega_0^2) [1 - \exp(-\frac{1}{2}\Delta^2 t^2) \cos(\omega_0 t)] + (2\Delta^4/\omega_0^3) \int_0^t \exp(-\frac{1}{2}\Delta^2 \tau^2) \sin(\omega_0 \tau) d\tau, \quad (6)$$

$$g_{+-}(t) \equiv \langle \sigma_+(t) \sigma_-(0) \rangle = (1 - \Delta^2/\omega_0^2) \exp(-\frac{1}{2}\Delta^2 t^2 - i\omega_0 t) + (i\Delta^2 t/\omega_0) \exp(-\frac{1}{2}\Delta^2 t^2 - i\omega_0 t) - (\Delta^4/\omega_0^3) \int_0^t \exp(-\frac{1}{2}\Delta^2 \tau^2) \sin(\omega_0 \tau) d\tau + \Delta^2/\omega_0^2, \quad (7)$$

where $\omega_0 = \gamma H_{\text{in}}$. The relaxation functions in the static limit are simply the Fourier transform of (6) and (7), and are given by

$$f_{zz}^0(\omega) = (1 - 2\Delta^2/\omega_0^2)/i\omega + 2\Delta^4 a(i\omega)/i\omega_0^3 \omega + \Delta b(i\omega)/\omega_0^2, \quad (8)$$

and

$$f_{+-}^0(\omega) = (1 - \Delta^2/\omega_0^2)(\pi/2)^{1/2} W[\omega_0 - \omega]/\sqrt{2}\Delta + (i/\omega_0) \{1 - i(\omega_0 - \omega)(\pi/2)^{1/2} W[(\omega_0 - \omega)/\sqrt{2}\Delta]/\Delta\} - [\Delta^4 a(i\omega)/i\omega_0^3 \omega + \Delta^2/\omega_0^2 \omega], \quad (9)$$

where

$$a(z) = (\sqrt{\pi}/2\sqrt{2}) i \Delta \{ W[(iz + \omega_0)/\sqrt{2}\Delta] - W[(iz - \omega_0)/\sqrt{2}\Delta] \}, \quad (10)$$

$$b(z) = (\sqrt{\pi}/2\sqrt{2}) \Delta \{ W[(iz + \omega_0)/\sqrt{2}\Delta] + W[(iz - \omega_0)/\sqrt{2}\Delta] \}, \quad (11)$$

and $W(z)$ is the complex error function.

In order to include fluctuations in the random fields, we employ the "strong-collision" model¹¹ of Hayano *et al.* In the fast-modulation (large- ν) regime, this result agrees with the diffusion method of Kubo and Toyabe.¹⁰ However, the diffusion method is not amenable to direct calculation in the low-field, slow-modulation limit, required here. By strong-collision dynamics, we mean that the system is viewed as developing in time in a random, but static field, and then jumping after a mean time ν^{-1} to a new configuration of static fields. In fact, our current picture of a spin glass, in which large blocks of spins make infrequent jumps between nearly equivalent, metastable states, conforms well to the strong collision model. The statistical independence of the random field configurations before and after the jump was exploited by Hayano *et al.* to derive averaged relaxation functions for fluctuating random fields in terms of those for static random fields. Because we are interested in the frequency dependence, we have used the analytic properties of the complex error function to continue the results of Hayano *et al.* to complex frequencies. The final results are

$$F_{zz}(\omega, \nu) = f_{zz}^0(\omega - i\nu) / [1 - \nu f_{zz}^0(\omega - i\nu)], \quad (12)$$

$$F_{+-}(\omega, \nu) = f_{+-}^0(\omega - i\nu) / [1 - \nu f_{+-}^0(\omega - i\nu)]. \quad (13)$$

Then, the transverse line $I_{xx}(\omega_0, \Delta, \nu)$ and the longitudinal line $I_{zz}(\omega_0, \Delta, \nu)$ can be expressed in terms of these relaxation functions as

$$I_{xx}(\omega_0, \Delta, \nu) = (1/4\pi) \text{Re}[F_{+-}(\omega_0, \Delta, \nu) + F_{-+}(\omega_0, \Delta, \nu)], \quad (14)$$

$$I_{zz}(\omega_0, \Delta, \nu) = (1/2\pi) \text{Re}F_{zz}(\omega_0, \Delta, \nu), \quad (15)$$

where $F_{-+}(\omega_0, \Delta, \nu) = F_{+-}(-\omega_0, \Delta, \nu)$. Therefore, the theoretical line shapes can be produced by evaluating numerically the relaxation functions. Note that a longitudinal absorption mode is predicted from this model as a result of the static splitting induced in the slow-modulation limit.

In the spin-glass regime, the position of the resonance has been predicted to shift from $H_R = \omega/\gamma$ to⁷

$$\omega = \frac{1}{2}\omega_r + \frac{1}{2}(\omega_r^2 + 4\omega_i^2)^{1/2}, \quad (16)$$

where $\omega_i/\gamma = \sqrt{K/\chi}$ is the anisotropy field and $\omega_r/\gamma = H_R$ is the resonance field. To treat this, we linearize (16) by introducing $\omega_a = \omega - \omega_r^{to}$ represent the shift in center frequency and take for the line shape

$$I_{xx}(\omega_0, \Delta, \nu, \omega_a) = \frac{1}{4\pi} \text{Re}\{F_{+-}[(\omega_0 + \omega_a), \Delta, \nu] + F_{-+}[(\omega_0 - \omega_a), \Delta, \nu]\}. \quad (17)$$

This choice guarantees that the absorption signal is symmetric in the applied field ω_0/γ , as it must be. The width Δ and relaxation rate ν are associated with ω_d and τ_{eff}^{-1} , respectively, in the conventional exchange narrowing model. However, it must be emphasized that the width and position agree with the extreme-narrowing limit used

previously by us and others only when $\Delta/\nu \ll 1$, a condition that is not met close to T_f .

IV. DATA ANALYSIS

Fitting the ESR data with the theoretical resonance lines of the Kubo-Toyabe model, we determine the parameters of interest: the relaxation rate ν , the rms width of the random local fields Δ , and the additional shift ω_a in the spin-glass phase, from which we can extract the static anisotropy field ω_i . The solid lines in Figs. 1 and 2 represent fits to the data above, near, and below T_f . The data and fitting functions have been normalized to unity at the maximum absorption. The fitting function includes a baseline value since the extreme broadening does not permit an accurate determination of the baseline at either high or low fields.

The line-shape function was calculated numerically using standard programs for the complex error functions. The parameters were varied within a standard least-squares fitting routine to obtain values of the parameters. Above T_f , suitable fits were obtained with $\omega_a = 0$, indicating that both the broadening and shift can be explained by purely dynamical effects. Below T_f , however, the shift greatly exceeds the broadening, and fits can only be obtained for $\omega_a \neq 0$.

The relaxation rate at both 9.3 and 1.1 GHz, as seen in Figs. 3 and 4, respectively, decreases strongly as the temperature approaches T_f . The data can be fitted by $\nu = c(T - T_f)$ for $T \geq 1.15T_f$. For both samples $c = 9.1 \times 10^9 \text{ s}^{-1} \text{ K}^{-1}$ at 9.3 GHz and $c = 2.95 \times 10^{10} \text{ s}^{-1} \text{ K}^{-1}$ at 1.1 GHz. Below $T = 1.15T_f$, ν decreases more slowly as the temperature is reduced and has a nonzero value at T_f . It is surprising that c is strongly field dependent. This effect has been noted previously and taken as evidence against a dynamical origin for the

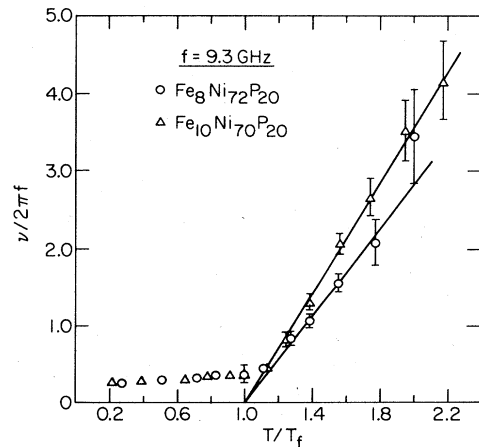


FIG. 3. The relaxation rate ν at 9.3 GHz is a linear function of temperature for $T \geq 1.15T_f$, $\nu = c(T - T_f)$, where $c = 9.1 \times 10^9 \text{ s}^{-1} \text{ K}^{-1}$ for both samples. It has a nonzero value at T_f and decreases slowly with temperature in the spin-glass phase.

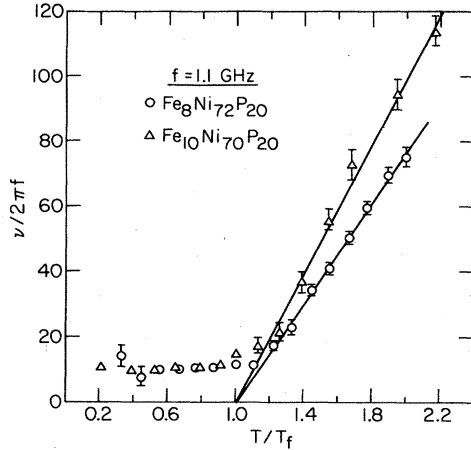


FIG. 4. The temperature dependence of the relaxation rate ν at 1.1 GHz is similar to that at 9.3 GHz. $\nu = c(T - T_f)$ for $T \geq 1.15T_f$, where $c = 2.95 \times 10^{10} \text{ s}^{-1} \text{ K}^{-1}$ for both samples.

shift and broadening. We note that the change in relaxation rate scales approximately as $H_R^{-1/2}$, although it is dangerous to take this seriously with only two frequency points.

The width Δ of the random field distribution at both 9.3 and 1.1 GHz shows an approximately χ^{-1} temperature dependence as seen in Figs. 5 and 6, respectively. For both samples, it is roughly frequency independent for $T \geq T_f$. Below T_f , the rms value Δ at 1.1 GHz is only slightly larger than that at 9.3 GHz. The field independence of Δ indicates that the magnitude of the random local fields, from the anisotropic interaction between spins in the spin system, is little affected by external field, while the dynamics, characterized by ν , are strongly affected.

The temperature dependence of ω_a at 9.3 and 1.1 GHz is shown in Figs. 7 and 8, respectively. As expected, ω_a is zero in the paramagnetic phase but, in the spin-glass

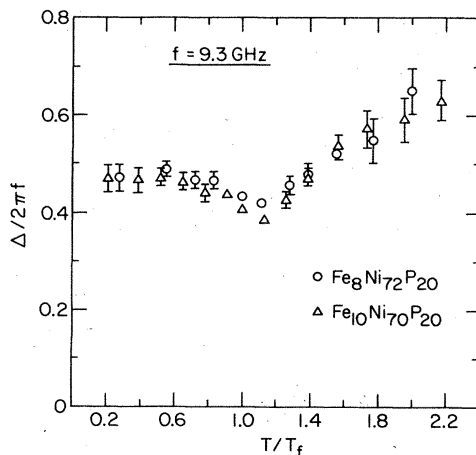


FIG. 5. The rms amplitude of random local fields Δ at 9.3 GHz has an approximately χ^{-1} temperature behavior for both samples.

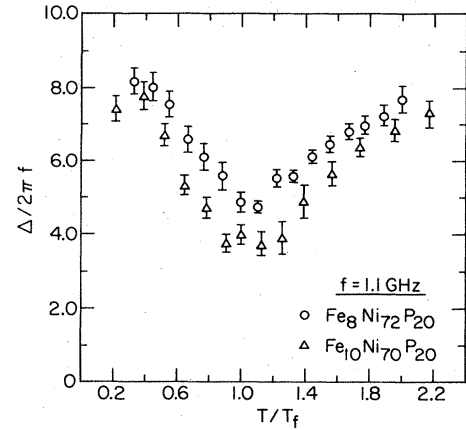


FIG. 6. The rms amplitude of random local fields Δ at 1.1 GHz has an approximately χ^{-1} temperature behavior for both samples and it is approximately equal to that at 9.3 GHz for $T \geq T_f$.

phase, increases as the temperature reduced. From the definition of ω_a , it is simple to show that

$$\omega_a \cong \begin{cases} \omega_i^2/\omega, & \omega_a < \omega \\ \omega_i, & \omega_a \gtrsim \omega \end{cases} \quad (18a)$$

$$(18b)$$

Barnes¹⁸ has argued that ω_i^2 is proportional to the spin-glass order parameter $q \sim (1 - T/T_f)$, while Sompolinsky *et al.*¹⁹ have shown the static anisotropy constant to be proportional to q^3 . However, in this model the anisotropy is a remanent effect, and its behavior depends on the time scale of the measurement. If the anisotropy frequency we observe were dominated by the remanent susceptibility,

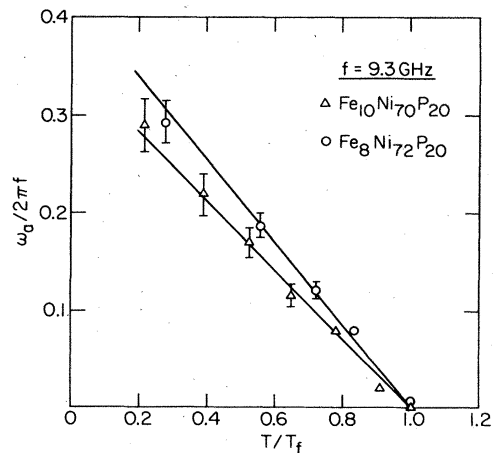


FIG. 7. The additional shift ω_a at 9.3 GHz has a zero value in paramagnetic phase, but $\omega_a = k(1 - T/T_f)$ in the spin-glass phase, where $k = 2.5 \times 10^{10} \text{ s}^{-1}$ for $\text{Fe}_8\text{Ni}_{72}\text{P}_{20}$ and $k = 2.1 \times 10^{10} \text{ s}^{-1}$ for $\text{Fe}_{10}\text{Ni}_{70}\text{P}_{20}$.

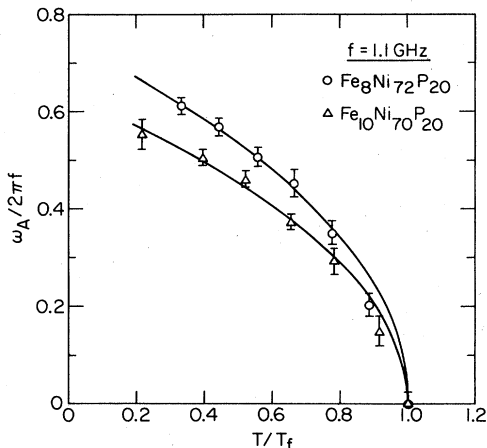


FIG. 8. The additional shift ω_a at 1.1 GHz also has a zero value in paramagnetic phase. $\omega_a \approx k(1 - T/T_f)$ as $\omega_a < 0.5 \omega$, where $k = 1.1 \times 10^{10} \text{ s}^{-1}$ for $\text{Fe}_8\text{Ni}_{72}\text{P}_{20}$ and $k = 8.8 \times 10^9 \text{ s}^{-1}$ for $\text{Fe}_{10}\text{Ni}_{70}\text{P}_{20}$. ω_a changes to $q^{1/2}$ behavior for $\omega_a > 0.5 \omega$, where q is the spin-glass order parameter and $q \sim (1 - T/T_f)$.

then the result of Sompolinsky *et al.* would also give a linear dependence on q . Close to T_f , we find that $\omega_a \approx k(1 - T/T_f)$, with $k \approx 2.1 \times 10^{10} \text{ s}^{-1}$ and $2.5 \times 10^{10} \text{ s}^{-1}$ at 9.3 GHz for $\text{Fe}_{10}\text{Ni}_{70}\text{P}_{20}$ and $\text{Fe}_8\text{Ni}_{72}\text{P}_{20}$, respectively. At 1.1 GHz, the linear regime is smaller, but we estimate $k \approx 8.8 \times 10^9 \text{ s}^{-1}$ and $1.1 \times 10^9 \text{ s}^{-1}$ for the two samples, respectively. Our data support the argument that the anisotropy frequency is linear in the spin-glass order parameter. The tendency for the anisotropy to increase with applied field was also predicted by Sompolinsky *et al.*¹⁹ Note that ω_a changes behavior when $\omega_a/\omega \geq 0.5$, as expected from (18b). Writing $K(0) = k\omega\chi/\gamma^2$, we find $K(0)$ to be 8.8×10^3 and $9.5 \times 10^3 \text{ ergs/cm}^3$ at 9.3 CHZ, and 3.9×10^3 and $4.0 \times 10^3 \text{ ergs/cm}^3$ at 1.1 GHz for $\text{Fe}_8\text{Ni}_{72}\text{P}_{20}$ and $\text{Fe}_{10}\text{Ni}_{70}\text{P}_{20}$, respectively.

V. DISCUSSION

In order to make contact with the phenomenological parameters Δ and ν of the Kubo-Toyabe theory, a microscopic model is required. The calculation of Levy *et al.* for the Mori-Kawasaki parameters may be used to determine Δ and ν as well. We take the random fields of the Kubo-Toyabe model to be the same as those induced by the Dzyaloshinsky-Moriya interaction and study the time development of their correlator. We find that the Levy *et al.* approach predicts a constant value of Δ for $T > T_f$ while ν decreases toward finite value at T_f . The temperature dependence is not as strong as observed.

More recent studies¹⁷ of spin-glass dynamics indicate that spin correlations exhibit power-law, rather than exponential, decay. If this is so, then there is no obvious characteristic time with which to associate ν^{-1} or τ_{eff} .

One possibility is that the most important Fourier component of the power spectrum is that at the Zeeman frequency. If this were so, then the characteristic time might scale with a power of the Zeeman frequency. The square-root dependence we see in our limited frequency-dependent data support this possibility.

An important effect, almost always ignored in ESR studies of spin glasses, is the dramatic change in line shape.¹⁵ Generally, this has been taken into account by arbitrarily changing the proportion of dispersion and absorption (mixing ratio) in the fits.³ There is no justification for doing this. Rather, these line-shape distortions signal important changes in the spin dynamics, from fast modulation (exchange narrowing) to the slow modulation described here. It is one of the most significant successes of the Kubo-Toyabe approach that it explains in detail the line-shape changes we have observed.

The combination of the derivative technique and severe distortion of the line can lead to spurious results. Using thick samples and field modulation at the temperature of c , Fig. 1, we found anomalous low-field modes. These do not represent new modes of the system, but rather the results of the zero-field absorption evident in c , Fig. 1 combined with skin-effect mixing. We recommend caution in interpreting resonance curves such as those in Ref. 6 to be due to a second mode.

In summary, the Kubo-Toyabe dynamics described here provide a detailed phenomenological description of the ESR data above T_f , including the shift in resonance position, linewidth, and line shape, using only two parameters. The parameters are qualitatively the same as those determined by Levy *et al.* from the simpler Mori-Kawasaki formalism, and strongly support our earlier assertion that exchange narrowing plays an important role. An unusual feature is the rather strong field dependence of the relaxation parameter which gives a slower relaxation at higher spectrometer frequencies (applied fields). We have suggested that this results from the mapping of power-law decays appropriate for the spin-glass problem onto the exponential decay assumed in the dynamical models. An effort is presently underway to extend the Kubo-Toyabe approach to more general forms for the relaxation of local fields. Finally, inclusion of dynamical effects accounts for all the shift in resonance position for $T > T_f$. Failure to do so results in an anisotropy field that extends above T_f . Clearly, a proper treatment of spin dynamics in spin-glass systems will have to consider both static anisotropy and the persistence of fluctuating local fields below T_f .

ACKNOWLEDGMENTS

We are deeply grateful to John L. Walter at General Electric Research Company for providing the samples. This work was supported through National Science Foundation Grant No. DMR-82-05484 with facility support by the University of Illinois Materials Research Laboratory.

- ¹R. Rammal and J. Souletie, in *Magnetism of Metals and Alloys*, edited by M. Cyrot (North-Holland, Amsterdam, 1982), p. 379.
- ²M. B. Salamon, *Solid State Commun.* **31**, 781 (1979); *J. Magn. Magn. Mater.* **15-18**, 197 (1980).
- ³G. Mozurkewich, J. H. Elliot, M. Hardiman, and R. Orbach (unpublished).
- ⁴P. M. Levy, C. Morgan-Pond, and R. Raghavan, *Phys. Rev. Lett.* **50**, 1160 (1983).
- ⁵H. Mori, in *Many Body Theory*, edited by R. Kubo (Benjamin, New York, 1966), p. 17.
- ⁶S. Schultz, E. M. Gullikson, D. R. Fredkin, and M. Tovar, *J. Appl. Phys.* **52**, 1776 (1981).
- ⁷C. L. Henley, H. Sompolinsky, and B. I. Halperin, *Phys. Rev. B* **25**, 5849 (1982).
- ⁸W. M. Saslow, *Phys. Rev. Lett.* **48**, 505 (1982).
- ⁹P. Monod, J. Cowan, H. Hurdequint, C. L. Henley, and W. M. Saslow (unpublished).
- ¹⁰R. Kubo and T. Toyabe, in *Magnetic Resonance and Relaxation*, edited by R. Blinc (North-Holland, Amsterdam, 1967), p. 810.
- ¹¹R. S. Hayano, Y. J. Uemura, J. Imazato, N. Nishida, T. Yamazaki, and R. Kubo, *Phys. Rev. B* **20**, 850 (1979).
- ¹²M.-K. Hou, M. B. Salamon, and T. A. L. Ziman, *J. Appl. Phys.* **55**, 1723 (1984).
- ¹³M. B. Salamon and J. L. Tholence, *J. Magn. Magn. Mater.* **31-34**, 1375 (1983).
- ¹⁴Y. Yeshurun, K. V. Rao, M. B. Salamon, and H. S. Chen, *J. Appl. Phys.* **52**, 1747 (1981).
- ¹⁵F. R. Hoekstra, K. Baberschke, M. Zomack, and J. Mydosh, *Solid State Commun.* **43**, 109 (1982).
- ¹⁶C. Kittel, in *Introduction to Solid State Physics*, 4th edition (Wiley, New York, 1976), p. 599.
- ¹⁷H. Sompolinsky and A. Zippelius, *Phys. Rev. Lett.* **47**, 359 (1981).
- ¹⁸S. E. Barnes, *Phys. Rev. Lett.* **47**, 1613 (1981).
- ¹⁹H. Sompolinsky, G. Kotliar, and A. Zippelius, *Phys. Rev. Lett.* **52**, 392 (1984).